Receptor-mediated hydrolysis of plasma membrane messenger PIP_2 leads to K^+-current desensitization

Evgeny Kobrinsky*, Tooraj Mirshahi*†, Hailin Zhang*, Taihao Jin* and Diomedes E. Logothetis*‡

*Departments of *Physiology & Biophysics and †Medicine, Mount Sinai School of Medicine of the New York University, New York, New York 10029, USA*
‡e-mail: Logothetis@msvax.mssm.edu

Phosphatidylinositol bisphosphate (PIP_2) directly regulates functions as diverse as the organization of the cytoskeleton, vesicular transport and ion channel activity. It is not known, however, whether dynamic changes in PIP_2 levels have a regulatory role of physiological importance in such functions. Here, we show in both native cardiac cells and heterologous expression systems that receptor-regulated PIP_2 hydrolysis results in desensitization of a GTP-binding protein-stimulated potassium current. Two receptor-regulated pathways in the plasma membrane cross-talk at the level of these channels to modulate potassium currents. One pathway signals through the βγ subunits of G proteins, which bind directly to the channel. Gβγ subunits stabilize interactions with PIP_2 and lead to persistent channel activation. The second pathway activates phospholipase C (PLC) which hydrolyses PIP_2 and limits Gβγ-stimulated activity. Our results provide evidence that PIP_2 itself is a receptor-regulated second messenger, downregulation of which accounts for a new form of desensitization.

Cellular excitability can be retarded by activation of G-protein-gated inwardly rectifying potassium (GIRK) channels (see, for example, refs 1–3), found in atrial and pacemaker cardiac cells, central neurons and endocrine cells. In the heart, acetylcholine (ACh) signals through G proteins to regulate the activity of GIRK channels and slow heart rate. In general, M_1 muscarinic receptors (as well as M_3 and M_5) typically couple to the $G_q\alpha$/11 family to stimulate effectors such as PLC, whereas M_2 receptors (as well as M_4) couple via the pertussis toxin (PTX)-sensitive G_i and G_o subunits to stimulate effectors such as GIRK channels (for review see ref. 4). Stimulation of GIRK currents is known to proceed through M_2 muscarinic receptors, causing activation of PTX-sensitive G proteins that leads to dissociation of the heterotrimeric complex into α and βγ subunits. In turn, the βγ dimers interact directly with the GIRK channels to stimulate their activity (see, for example, refs 5–7). In response to a sustained exposure to ACh (for example 100 μM), atrial cells exhibit K^+ current activation that reaches a peak (p_1) within several hundred milliseconds and gradually decreases to a quasi-steady-state (qss) level within 1 min (Fig. 1a). This characteristic reduction of K^+ current in the continuous presence of ACh is independent of receptor desensitization and has been referred to as 'short-term' desensitization[8]. A second brief exposure to ACh yields a response with a reduced peak (p_2), indicating lack of recovery from desensitization. The molecular mechanisms of GIRK current desensitization have not yet been established.

Results

PLC-mediated hydrolysis of PIP_2 results in K^+ current desensitization in rat atrial cells. Block of the G_q pathway at the receptor, G protein or effector levels in an atrial myocyte greatly attenuated K^+ current desensitization (Fig. 1). The M_1 antagonist pirenzepine (1 μM) had no effect on current desensitization (Fig. 1b). In contrast, the M_3 antagonist 4-DAMP mustard hydrochloride (4-DAMP; 0.5 μM) largely inhibited current desensitization and yielded responses of comparable magnitude to that observed between the first and second ACh applications (Fig. 1c). This result suggested that the ACh-induced desensitization involved M_3 and not M_1 muscarinic receptors in atrial cells. A control peptide, ADRK, included in the pipette solution, did not significantly affect the desensitization characteristics of the K^+ current (Fig. 1d)[9]. In contrast, when we included in the patch pipette the peptide QLKK, which has been shown to block $G_q\alpha$-mediated activation of PLC[9], there was a greatly reduced decline in current between peak and quasi-steady-state levels, and the second response to ACh was comparable in magnitude to the first (Fig. 1e). Moreover, treatment of an atrial myocyte with the PLC inhibitor U73122 (1 μM) had similar inhibitory effects on the desensitization process (Fig. 1f). Summary data, comparing control conditions versus a block of PLC with U73122, a block of $G_q\alpha$ with the QLKK peptide, or a block of M_3 receptors by 4-DAMP, showed significantly increased quasi-steady-state to peak ratios (Fig. 1g). Summary data of the ratio of the second to first peak current responses to ACh also showed a significant increase as a result of a block by either the M_3 antagonist or the blockers of $G_q\alpha$ or PLC (Fig. 1h). These results suggest that the K^+ current desensitization seen in native atrial myocytes involves M_3 receptor stimulation of a G_q pathway leading to activation of PLC.

Current desensitization through PLC-mediated hydrolysis of PIP_2 in COS-1 cells. We next turned to heterologous expression systems, where signalling through particular G-protein-coupled pathways can be controlled by expressing the proteins involved. We performed whole-cell recordings in COS-1 cells co-expressing GIRK channel subunits and M_2 receptor with or without M_1 receptor (Fig. 2). We used M_1 receptor to activate the G_q pathway because in our hands heterologous expression of this receptor yielded robust responses. Application of 5 μM ACh on a cell expressing M_2 receptor alone resulted in a macroscopic current with small changes between peak and quasi-steady-state levels (Fig. 2a, left panel). A second application of ACh yielded a similar response (Fig. 2a, right panel). In contrast, in cells expressing both M_1 and M_2 receptors, ACh elicited currents that showed a marked decline between peak and quasi-steady-state levels, suggesting K^+-current desensitization (Fig. 2b, left panel). A second ACh application yielded a very small response, suggesting that K^+ currents had not yet recovered from desensitization (Fig. 2b, right panel). Blocking PLC activity with U73122 before the application of ACh largely prevented M_1-receptor-mediated desensitization of K^+ currents (Fig. 2c, left panel). Additionally, in cells treated with U73122 (1 μM) a second application of ACh resulted in comparable currents to those elicited by the first ACh application (Fig. 2c, right panel). Summary data of the

© 2000 Macmillan Magazines Ltd

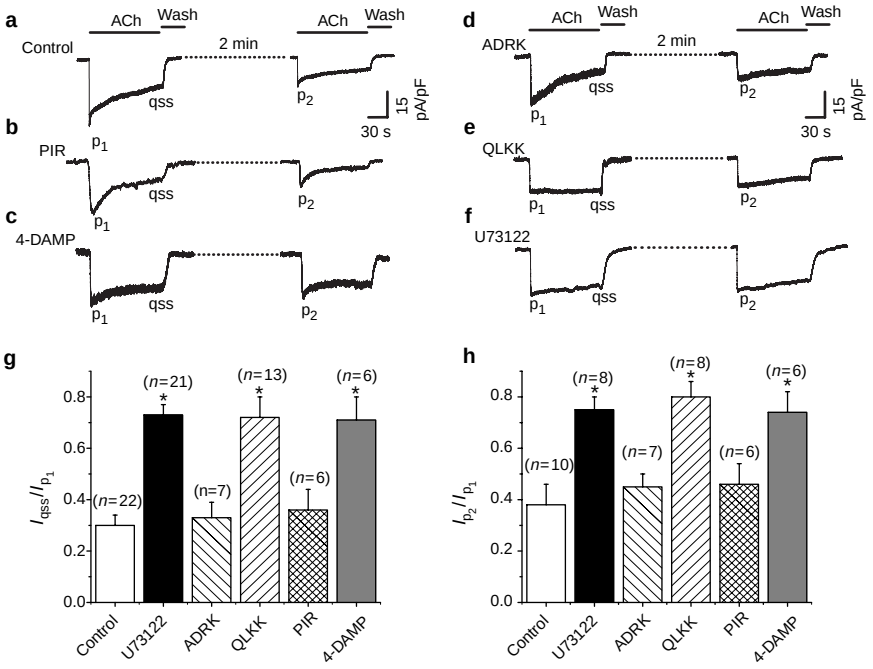

Figure 1 **Blocking receptor, $G_q\alpha$ or PLC attenuates K^+ current desensitization in rat atrial myocytes. a**, ACh (100 μM) induced K^+ currents (K_{ACh}) in neonatal rat atrial cells. Peak (p_1 and p_2) and quasi-steady-state (qss) levels of K_{ACh} currents are indicated. The second application of ACh was 2 min after washout of the first. **b**, Pirenzepine (PIR, 1 μM) did not affect the desensitization properties of the K_{ACh} current. **c**, 4-DAMP mustard hydrochloride (4-DAMP, 0.5 μM) significantly attenuated desensitization of the muscarinic K^+ current. **d**, Inclusion of 50 μM control peptide, ADRK, in the pipette did not affect K^+ current desensitization following equilibration of the patch solution with that of the cell interior. **e**, Inclusion of 50 μM QLKK peptide in the pipette greatly attenuated K^+ current desensitization following equilibration of the patch solution with that of the cell interior. **f**, Recordings were obtained under similar conditions as in **a**, except that U 73122 (1 μM) was applied 2 min before agonist application. **g**, Histogram showing the ratio of quasi-steady-state to peak levels of K_{ACh} currents. Control, 0.30 ± 0.04; U73122, 0.73 ± 0.04; ADRK, 0.33 ± 0.06; QLKK, 0.72 ± 0.08; PIR, 0.36 ± 0.08; 4-DAMP, 0.71 ± 0.09; $P < 0.0001$. Peak and quasi-steady-state currents were measured with reference to the pre-ACh-stimulated currents. **h**, Histogram showing the ratio of the amplitudes of the second to first peak current responses to ACh (100 μM). Control, 0.38 ± 0.08; U73122, 0.75 ± 0.05; ADRK, 0.45 ± 0.05; QLKK, 0.8 ± 0.06; PIR, 0.46 ± 0.08; 4-DAMP, 0.74 ± 0.08; $P < 0.01$.

ratio of quasi-steady-state to peak currents for M_2 (alone), M_1+M_2 and M_1+M_2 preincubated with U73122 show that stimulation of the M_1 receptor causes a significant decline in ACh-induced K^+ currents that can be prevented by the PLC inhibitor (Fig. 2d). Fig. 2e plots the ratio of peak currents elicited by the second versus the first ACh stimulation. A significant decrease in the amplitude of the second ACh-induced current was obtained when M_1 receptor was present, an effect that could again be prevented by U73122. These results show that activation of PLC through the M_1 receptor can mediate GIRK current desensitization.

Signalling through the M_1 receptor caused PLC-mediated PIP_2 hydrolysis in COS-1 cells. Recent studies have utilized fluorescence measurements to describe the dynamic nature of PIP_2 hydrolysis through signalling pathways that lead to activation of PLC. These studies have used a pleckstrin homology (PH) domain of PLC-δ tagged with green fluorescent protein (GFP–PH)[10–12]. GFP–PH is a powerful tool for monitoring PIP_2 hydrolysis but, as it binds specifically to both inositol trisphosphate (IP_3) and PIP_2, it provides a relative rather than an absolute measurement of changes in plasma membrane PIP_2 levels[12]. We expressed channels and receptors with GFP–PH in COS-1 cells and used confocal microscopy to quantify PIP_2 hydrolysis. Representative field images of COS-1 cells co-expressing GIRK1 and GIRK4 subunits, muscarinic receptor(s) and GFP–PH are shown (Fig. 3a). Quantitative analysis of the relative fluorescence in the membrane versus the cytosol is also shown (Fig. 3b). When the M_2 receptor was expressed, images before and after receptor stimulation with ACh (5 μM) showed no significant translocation of fluorescence signal from the plasma membrane to the cytoplasm (Fig. 3a (top) and 3b). In contrast, cells expressing M_1 and M_2 receptors together showed a reversible translocation of the fluorescence signal in response to ACh. This suggested rapid hydrolysis (monitored as early as 15 seconds following ACh application) with a slower recovery phase of the fluorescence signal (Fig. 3a (middle) and 3b). When these M_1M_2-expressing cells were incubated with the PLC inhibitor U73122 (1 μM) for 3 min before ACh application, GFP translocation was significantly attenuated, indicating that inhibition of PLC activity greatly reduced the M_1-triggered hydrolysis of PIP_2 (Fig. 3a (bottom) and 3b). These results indicate that stimulation of heterologously expressed M_1 but not M_2 receptors caused hydrolysis of PIP_2 that could largely be inhibited by the PLC inhibitor U73122. The GFP–PH translocation data together with the electrophysiological results argue strongly that M_1 receptor stimulation leads to PLC-mediated hydrolysis of PIP_2, resulting in K^+ current desensitization in a mammalian heterologous expression system. Thus, muscarinic stimulation involves a mixed response of two pathways: one that activates K^+ currents through Gβγ subunits and another leading to PLC-mediated hydrolysis of PIP_2 and current desensitization.

M_1 receptor signalling inhibits M_2-receptor-induced K^+ currents in *Xenopus laevis* oocytes. The *Xenopus* oocyte system enabled us to simultaneously monitor hydrolysis of PIP_2 and its effects on GIRK currents. We simultaneously monitored endogenous outwardly rectifying Ca^{2+}-activated Cl^- currents and expressed inwardly rectifying GIRK currents. We co-expressed GIRK channels in oocytes together with M_1 or M_2 receptors, individually or in combination, and characterized ACh-induced effects on GIRK and Ca^{2+}-activated Cl^- channel activity. In a recording from an oocyte expressing the M_2 receptor

© 2000 Macmillan Magazines Ltd

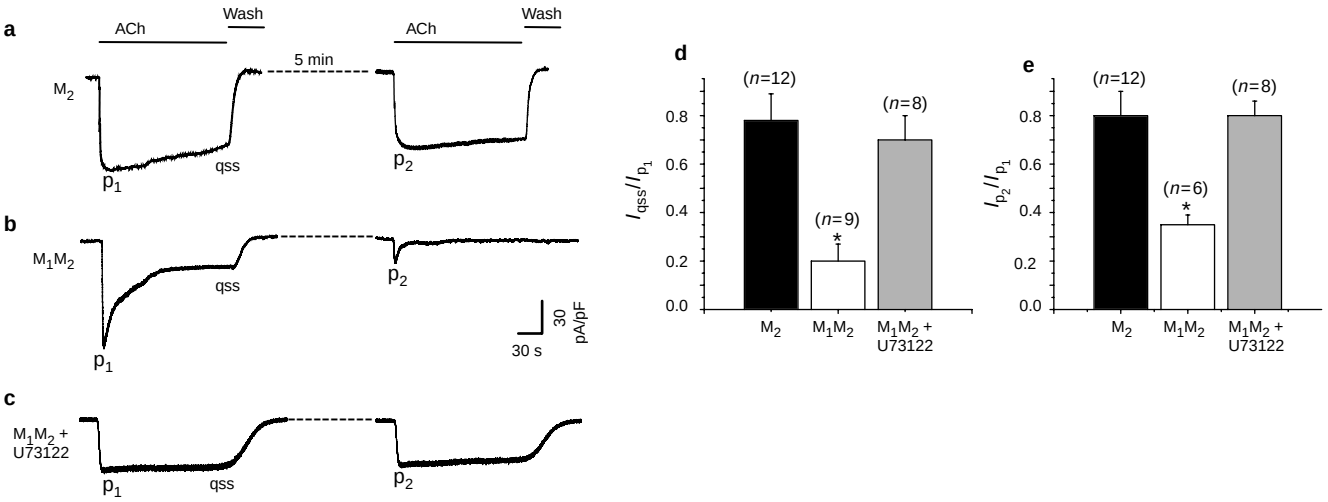

Figure 2 **PLC activation via M_1 receptor stimulation in COS-1 cells results in rapidly desensitizing GIRK currents. a**, Application of 5 μM ACh for 3 min induced potassium currents in COS-1 cells expressing M_2 receptor and GIRK1/GIRK4 channel subunits. Peak (p 1, p 2) and quasi-steady-state (qss) current levels are indicated. Currents were recorded at a holding potential of –80 mV. The second ACh application was 5 min after washout of the first. **b**, Recordings of ACh-induced K^+ currents in COS-1 cells expressing M_1 and M_2 receptors and GIRK1/GIRK4 channel subunits. **c**, Recordings of ACh-induced potassium currents in COS-1 cells expressing M_1 and M_2 receptors and GIRK1/GIRK4 channel subunits as in **b**, but following 2 min pretreatment with U73122 (1 μM). **d**, Histogram showing the ratio of the quasi-steady-state to peak levels of ACh-induced K^+ current. M_2, 0.78 ± 0.11; M_1M_2, 0.2 ± 0.07; M_1M_2 + U73122, 0.7 ± 0.1; $P < 0.005$ for comparison of M_2 versus M_1M_2. Peak and quasi-steady-state currents were measured with reference to the pre-ACh-stimulated currents. **e**, Histogram showing the ratio of the second to first ACh-induced peak current responses. M_2, 0.8 ± 0.1; M_1M_2, 0.35 ± 0.04; M_1M_2 + U73122, 0.8 ± 0.06; $P < 0.005$ for comparison of M_2 versus M_1M_2.

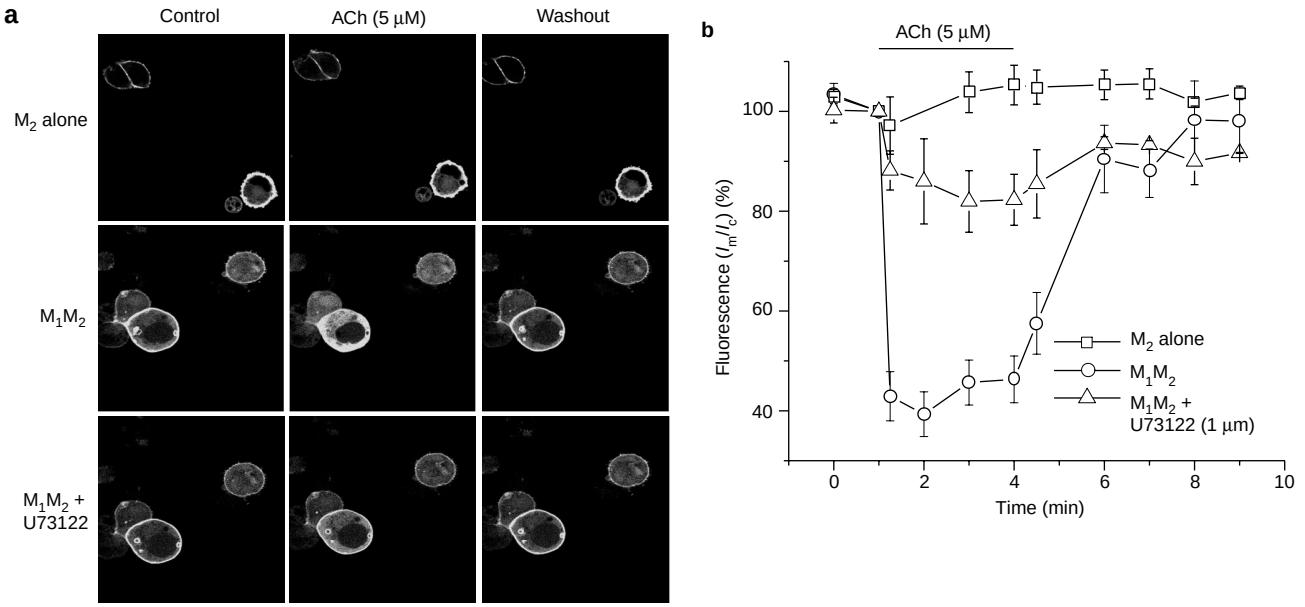

Figure 3 **PLC activation via M_1 receptor stimulation in COS-1 cells results in PIP_2 hydrolysis. a**, Selected representative field of COS-1 cells expressing the GFP–PH domain and specific muscarinic receptor(s). The images for Control, ACh and Washout correspond respectively to the 1, 3 and 9 min time points shown on the *x*-axis of **b**. ACh was applied at the 1 min time point in each case. When GFP–PH was co-expressed with the M_2 receptor, ACh (5 μM) did not induce PIP_2 hydrolysis. When GFP–PH was co-expressed with both the M_1 and M_2 receptors, ACh application led to PIP_2 hydrolysis, and washout of ACh reversed this effect. Preincubation of the cells with 1 μM U73122 for 3 min before ACh co-application inhibited the M_1-regulated PIP_2 hydrolysis. **b**, Quantitative analysis of the relative fluorescence in membrane (I_m) versus cytosol (I_c) in COS-1 cells (see Methods for details) expressing channels with M_2 receptors ($n = 4$) or M_1 and M_2 receptors without U73122 ($n = 6$) or with U73122 ($n = 3$).

© 2000 Macmillan Magazines Ltd

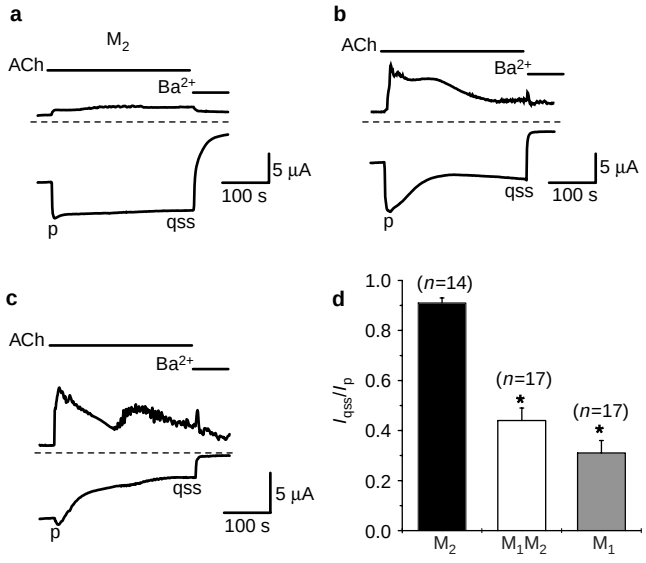

Figure 4 **M_1 receptor signalling causes inhibition of GIRK currents in *Xenopus laevis* oocytes.** ACh (5 µM) was applied for 300 s. Ba^{2+} (3 mM) was used to block GIRK currents at the end of the experiment. Dotted lines indicate the zero current line. **a**, A recording from a *Xenopus* oocyte expressing the M_2 receptor and GIRK1/GIRK4 channel subunits. Large and sustained inward GIRK currents were elicited by ACh. Peak GIRK currents obtained in the presence of ACh are marked at the beginning and end of the ACh application. p, peak; qss, quasi steady state. **b**, A recording of Ca^{2+}-activated Cl^- and GIRK1/GIRK4 currents from a *Xenopus* oocyte expressing M_1 and M_2 receptors and GIRK1/GIRK4 channel subunits. Conditions were the same as in **a**. Activation and inhibition of inward GIRK currents in the presence of ACh are marked respectively at the beginning (p) and end (qss) of the ACh application. **c**, A recording from a *Xenopus* oocyte expressing M_1 receptors and GIRK1/GIRK4 channel subunits. Conditions were the same as in **a**. ACh induced activation of oscillating Ca^{2+}-activated Cl^- currents and inhibition of inward basal GIRK currents. Peak (p) and quasi steady state (qss) are marked at the end of the ACh application. **d**, Histogram showing the ratio of the quasi-steady-state to peak levels of ACh-induced K^+ current. M_2, 0.91 ± 0.02; M_1M_2, 0.44 ± 0.05; M_1, 0.31 ± 0.05; $P < 0.0001$). Peak and quasi-steady-state currents were measured with reference to the current remaining after Ba^{2+} block.

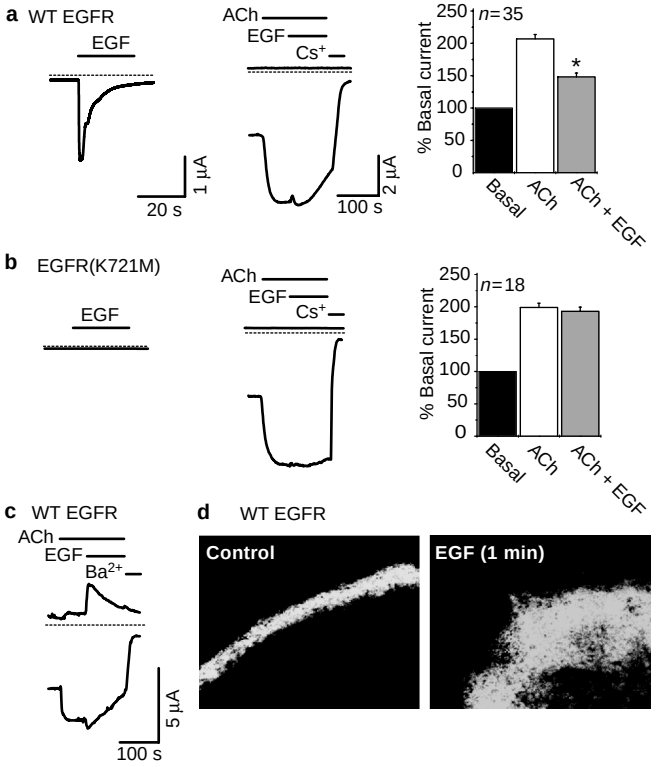

Figure 5 **Hydrolysis of PIP_2 through EGF receptor signalling causes inhibition of M_2-stimulated GIRK currents in *Xenopus* oocytes.** *Xenopus* oocytes were co-injected with cRNAs for EGFR, M_2 receptor and GIRK1/GIRK4 channel subunits. A two-electrode voltage clamp and confocal experiments were performed 2 days after injection. **a**, With wild-type (WT) EGFR, EGF (100 ng ml^{-1}) induced Ca^{2+}-activated Cl^- current in ND96 solution (left panel). The same oocyte was incubated for 3 h with 1 µM thapsigargin and 1 mM EGTA to deplete intracellular calcium stores before recording GIRK currents. The middle panel shows the K^+ current, which was recorded in high-potassium solution. Currents were monitored at –80 mV and + 80 mV at 1-s time intervals (see Methods). The histogram shows the ACh-induced (5 µM) increase in the potassium current and its inhibition by EGF as a percentage of the basal current. The currents were measured at the end of a 70-s application of ACh and a 100-s application of ACh + EGF. ACh, 207 ± 6.7%; ACh + EGF, 148 ± 6.2%; * denotes $P < 0.0001$, paired *t*-test. **b**, EGF effects on Ca^{2+}-activated Cl^- currents in *Xenopus* oocytes expressing a mutant, kinase-deficient EGFR, EGFR(K721M), instead of the wild-type EGFR (left panel). Recording of the K^+ current from the same thapsigargin-treated oocyte is shown in the middle panel. Conditions were the same as in Fig. 1a. The histogram shows the ACh-induced increase in the potassium current and the lack of effect of EGF in *Xenopus* oocytes expressing mutant EGFR as a percentage of the basal current. ACh, 199 ± 6.5%; ACh + EGF, 193 ± 6.7%; *P* is non-significant. **c**, A recording from an oocyte not treated with thapsigargin, where K^+ and Cl^- currents were monitored concurrently at both –80 and + 80 mV. Simultaneous monitoring of K^+ and Cl^- currents gave similar results to the experiments before and after treatment with thapsigargin (see Fig. 1a). Cs^+ was used instead of Ba^{2+}, as in these experiments EGTA was present. **d**, Expression of PH-GFP in an albino *Xenopus* oocyte expressing EGFR. The GFP construct localizes to the plasma membrane (left panel). Application of EGF (100 ng ml^{-1}) translocated the signal to the cytoplasm (right panel).

and channel subunits, ACh induced a small outward Ca^{2+}-activated Cl^- current and a simultaneous large and sustained inward K^+ current (Fig. 4a). Signalling through simultaneous stimulation of M_1 and M_2 produced a large Ca^{2+}-activated Cl^- current and an inward peak (p) agonist-induced K^+ current that gradually decreased to a quasi-steady-state (qss) level in the continued presence of ACh. This result suggested that the M_1 induction of PIP_2 hydrolysis caused reduction of the K^+ current but stimulation of the Ca^{2+}-activated Cl^- current, most likely through IP_3 production and Ca^{2+} release from intracellular stores (Fig. 4b). Finally, oocytes expressing channel subunits with the M_1 receptor alone in the continued presence of ACh showed a large outward Ca^{2+}-activated Cl^- current and an inward basal K^+ current that gradually decreased to a quasi-steady-state level. These results suggested M_1 induction of PIP_2 hydrolysis and inhibition of basal K^+ currents (Fig. 4c). Fig. 4d summarizes several such experiments by plotting the ratio of the quasi-steady-state to peak currents for oocytes expressing M_2, M_1+M_2 or M_1 receptors. Similar effects were observed in M_2-stimulated GIRK currents in oocytes treated with thapsigargin, which depletes Ca^{2+} stores[34], thus making dependence on Ca^{2+} signalling unlikely (I_{qss}/I_p for M_2 is 0.66 ±0.05, $n=25$ and for M_1+M_2 is 0.12±0.04; $n=22$; $P<0.0005$). Overall, these results show that in oocytes, as in COS-1 cells, signalling via M_1 receptors results in gradually decreasing GIRK currents.

G-protein-independent hydrolysis of PIP_2 inhibits ACh-induced k^+ currents. Can PLC-mediated hydrolysis of PIP_2 also result in K^+ current desensitization when it is induced independently of heterotrimeric G proteins? The epidermal growth factor receptor (EGFR) hydrolyses PIP_2 via direct coupling to PLCγ, allowing precise control of the timing of the induction of PIP_2 hydrolysis, inde-

© 2000 Macmillan Magazines Ltd

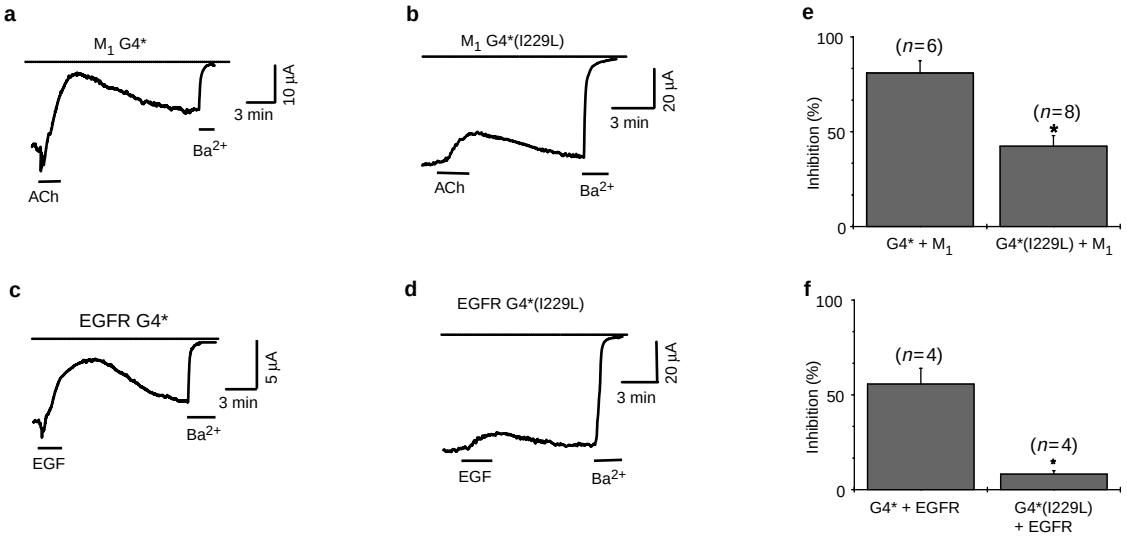

Figure 6 **An increase in the strength of GIRK4* channel- PIP_2 interactions reduces agonist-induced current inhibition in Xenopus oocytes. a**, M_1 stimulation (by ACh) inhibited GIRK4* (G4*) currents. ACh was applied to oocytes with stable G4* currents for a period of 170 s. ACh was then washed and the current recovered slowly. **b**, M_1 stimulation inhibited G4*(I229L) currents to a lesser degree than G4* currents. **c**, EGFR stimulation (by 100 ng ml^{-1} EGF) inhibited G4* currents. Conditions and responses were similar to those described in **a**. **d**, EGFR stimulation inhibited G4(I229L) currents to a lesser degree than G4* currents, as in **b**. **e**, Summary data for the inhibition of K^+ currents through G4* and G4*(I229L) respectively, by stimulation of M_1 receptor (percent inhibition 81 ± 6.5 vs 42.4 ± 5.6; n = 7, $P < 0.001$). **f**, Summary data for inhibition of K^+ currents of G4* and G4*(I229L) respectively, by stimulation of EGFR (percent inhibition 55.8 ± 8.3 vs 8.25 ± 1.8; n = 4, $P < 0.001$).

pendent of Gβγ-mediated effects (Fig. 5). GIRK subunits, M_2 muscarinic receptors and EGFR were co-expressed by injection of their cRNAs in *Xenopus* oocytes. In low external K^+ solutions, EGF induced transient Ca^{2+}-activated Cl^- currents that served as a positive control for EGF-induced hydrolysis of PIP_2 (Fig. 5a, left panel). This oocyte was next treated by thapsigargin to deplete Ca^{2+} stores and thus prevent activation of Ca^{2+}-activated Cl^- currents[34]. When the oocyte was then placed in high external K^+ solutions, basal K^+ currents developed. ACh (5 µM) induced and EGF (100 ng ml^{-1}) partially inhibited K^+ currents, which could be fully blocked by Cs^+ (10 mM) (Fig. 5a, middle panel). No outward Ca^{2+}-activated Cl^- currents were detected (at +80 mV), indicating the effectiveness of the thapsigargin treatment (compare Fig. 5c, in the absence of thapsigargin). Summary data show that the K^+ current is induced by ACh and inhibited by EGF (Fig. 5a, right panel). A kinase-deficient EGFR[13] served as a negative control for both stimulation of Cl^- current (Fig. 5b, left panel) and EGF-induced inhibition of GIRK current (Fig. 5b, middle panel). Summary data show that with the inactive EGFR, ACh-induced currents were not inhibited by EGF (Fig. 5b, right panel). As the actions of EGF on ACh-induced GIRK currents in the above experiments were tested on thapsigargin-treated Ca^{2+}-depleted oocytes, it appears that Ca^{2+} release was not necessary for the inhibitory effects of EGF observed. Ca^{2+}-activated Cl^- currents and GIRK currents were also measured simultaneously in oocytes that were not treated with thapsigargin (Fig. 5c). ACh again induced sustained inward GIRK currents at –80 mV. Addition of EGF induced large outward (+80 mV) and much smaller inward (–80 mV) Ca^{2+}-activated Cl^- currents. Moreover, EGF caused partial inhibition of GIRK currents that could be fully blocked by 3 mM Ba^{2+}. Experiments with U73122 attenuated EGF effects on the ACh-induced K^+ currents (data not shown). However, in oocytes, U73122 had to be used in higher concentrations (≥2 µM) than in mammalian cells in order to be effective. At these concentrations we found U73122 also inhibited basal GIRK currents. Experiments with the nonspecific PKC inhibitor staurosporine (2 µM) showed no effect on EGF inhibition of the ACh-induced GIRK currents (n =13), suggesting that PKC was not involved. Fig. 5d displays confocal images from an albino *Xenopus* oocyte expressing GFP–PH and EGFR. GFP–PH localized to the plasma membrane, where it bound to PIP_2 (Fig. 5d, left panel). Application of EGF (100 ng ml^{-1}) caused rapid translocation of the GFP signal to the cytoplasm, allowing direct observation of PIP_2 hydrolysis (Fig. 5d, right panel).

The strength of channel-PIP2 interactions determines the extent of agonist-induced current inhibition. The experiments utilizing heterologous expression of GIRK channels with specific receptors in either COS-1 cells or oocytes showed that PIP_2 hydrolysis occurred within seconds of stimulation, consistent with the kinetics of inhibition of the ACh-induced GIRK current. How does hydrolysis of PIP_2 result in GIRK current desensitization?

Functional studies on ion channels and transporters have shown that formation or hydrolysis of PIP_2 affects the activity of these proteins (for review see refs 14, 15). Inwardly rectifying K^+ (K_{ir}) channels have been shown to interact directly with PIP_2. PIP_2 interacts with GIRK channels weakly and at the low concentrations found in the plasma membrane it does not normally gate these channels. The effects of PIP_2 on the activity of GIRK channels are direct and are not mimicked by PIP_2 hydrolysis products[20–22]. PIP_2, produced via hydrolysis of ATP or applied exogenously, causes unitary channel openings to display two-to threefold longer open-state residence times than control[21,24]. Following this effect, the channel is sensitized to gating molecules or ions such as Gβγ or Na^+ (ref. 24). Gating molecules seem to stabilize channel interactions with PIP_2, suggesting that gating proceeds by modulating channel-PIP_2 interactions[21,22,25–27]. Although the dependence of inwardly rectifying K^+ channel activity on PIP_2 is striking, a physiological role for PIP_2 itself as a direct, receptor-regulated second messenger has not yet been established.

As Gβγ subunits require the presence of PIP_2 to stimulate and maintain activity of K^+ channels[21] we asked whether receptor-regulated hydrolysis of PIP_2 limits the direct interactions between GIRK and the phosphoinositide, leading to desensitization. We performed two types of experiments to address this question. First, we

© 2000 Macmillan Magazines Ltd

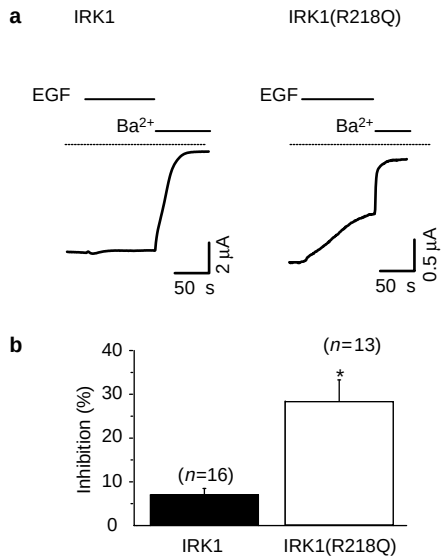

Figure 7 **A decrease in the strength of IRK1 channel-PIP$_2$ interactions confers agonist-induced current inhibition in *Xenopus* oocytes. a**, EGF (100 ng ml^{-1}) inhibited IRK1(R218Q) currents but not wild-type IRK1 currents in *Xenopus* oocytes expressing IRK1 channels and EGFR. Recordings were performed in thapsigargin-treated oocytes. **b**, Summary data for the inhibition of IRK1 currents by EGF (IRK1 inhibition was 7.0 ± 1.5%, and IRK1(R218Q) inhibition was 28.3 ± 5.0%; $P < 0.01$).

tested whether PLC-mediated PIP$_2$ hydrolysis that caused partial desensitization would reduce the channel open-time kinetics. We injected oocytes with GIRK1/GIRK4 channels and either M_2 or $M_1 + M_2$ receptor(s) and recorded unitary activity (from one or two individual channels) in the cell-attached mode with 10 μM ACh in the patch pipette. Open-time kinetics were fitted by two exponential components with time constants τ_{o1} and τ_{o2}. The M_2-expressing oocytes gave unitary openings with $\tau_{o1} = 1.22 \pm 0.05$ ms, $\tau_{o2} = 4.62 \pm 0.38$ ms and mean open time of 2.21 ± 0.12 ms ($n = 3$). The oocytes expressing $M_1 + M_2$ gave unitary openings with $\tau_{o1} = 1.12 \pm 0.09$ ms, $\tau_{o2} = 4.18 \pm 0.51$ ms and mean open time of 1.81 ± 0.28 ms ($n = 4$). Although the trend of the inhibitory effect seemed to be present, Student *t*-test of these measurements did not find them significantly different ($P = 0.29$). Thus, these results suggest that the PLC-mediated hydrolysis of PIP$_2$ was not sufficient in magnitude to produce a significant reduction in open-time kinetics.

We next tested the effects of PLC-mediated hydrolysis of PIP$_2$ on channel point mutants that exhibit altered interactions with PIP$_2$. We previously identified an amino acid difference between a highly active homotetrameric GIRK4 channel subunit (G4*) and the constitutively active channel IRK1, which is critical for interactions with PIP$_2$[22]. Mutation of isoleucine in G4*(I229) to the corresponding IRK1 leucine (L222) strengthened interactions with PIP$_2$, whereas the reverse mutation IRK1(L222I) weakened such interactions. We first used the G4*(I229L) point mutant that shows stronger interactions with PIP$_2$ than G4* (ref. 22). Fig. 6a shows a recording from an oocyte expressing M_1 receptor and G4* in which a brief ACh application reversibly inhibited G4* basal currents. ACh-induced inhibition of basal G4*(I229L) currents was markedly lower and took less time to recover than the effect on G4* currents (Fig. 6b). Similar responses were obtained when G4* and G4*(I229L) co-expressed with epidermal growth factor receptor (EGFR) were exposed to EGF (Fig. 6c, d). Summary data show that the level of the agonist-induced inhibition (Fig. 6e, f) differed significantly between G4* and G4*(I229L). Thus G4*(I229L), which interacts more srongly with PIP$_2$ than does G4*, is inhibited less by PIP$_2$ hydrolysis. These data strongly suggest that the PLC-mediated inhibition of K^+ currents proceeds through direct interactions of PIP$_2$ with GIRK channels.

IRK1 currents are not normally subject to agonist-induced inhibition. We previously identified two arginine residues, IRK1(R218) and IRK1(R228), that showed strong interactions with PIP$_2$. Neutralization of IRK1(R218) to glutamine, for example, showed a drastic decrease in interaction with PIP$_2$ and greatly diminished whole-cell currents[22]. We proceeded to test whether the R218Q mutation could confer agonist sensitivity on IRK1 currents by virtue of the decreased channel-PIP$_2$ interactions. Fig. 7a (left) shows that following co-expression of IRK1 with EGFR in *Xenopus* oocytes, application of EGF did not have a significant effect on IRK1 currents. In contrast, EGF significantly inhibited the IRK1(R218Q) mutant K^+ currents (Fig. 7a, right), suggesting that the weakened channel-PIP$_2$ interactions could allow hydrolysis of PIP$_2$ away from the channel. Summary data are shown in Fig. 7b. Therefore, we conclude that the extent of agonist-induced current inhibition of these inwardly rectifying K^+ channels is controlled by the strength of direct interactions between the channel and PIP$_2$.

Discussion

Even though direct interactions of PIP$_2$ with ion channels have been demonstrated in a number of isolated patch experiments, the key question has been whether the crucial dependence of channel activity on PIP$_2$ is under physiological regulatory control. Recently Xie and colleagues[28] provided electrophysiological evidence that PLC-linked receptors can regulate the ATP-sensitive K^+ currents by means of PIP$_2$ metabolism in heterologous expression systems. Our study provides compelling evidence that such regulation takes place not only in heterologous expression systems but in atrial myocytes, where PIP$_2$ hydrolysis underlies GIRK current desensitization. These results are intriguing on two counts: on the one hand they underscore the physiological importance of PIP$_2$ hydrolysis, and on the other they provide us with a novel mechanism for desensitization that does not involve receptor desensitization. We have shown that K^+ current desensitization can occur via agonist-induced regulation of PIP$_2$ hydrolysis in both cardiac cells and heterologous expression systems. Our results suggest that K^+ channel activity represents the balance of two pathways: one is stimulatory, signalling through Gβγ subunits that interact directly with the channel to stabilize interactions with PIP$_2$ leading to channel activation; the other pathway is inhibitory, activating PLC to hydrolyse PIP$_2$ and limit the stimulation of activity by Gβγ. Blocking the inhibitory component results in sustained currents in both heterologous expression systems and native atrial myocytes. It is important to stress that we have chosen one major way by which PIP$_2$ levels can be regulated to test the physiological significance of PIP$_2$ hydrolysis. This should not, however, be interpreted as the only way by which PIP$_2$ hydrolysis could have physiological consequences. Both synthesis and hydrolysis of PIP$_2$ are under the control of lipid kinases and phosphatases, which themselves can be regulated. Moreover, regulatory elements that affect the balance of the two pathways could affect desensitization. Examples of such complex regulatory influences may be the effects of intracellular application of a non-hydrolysable GTP analogue[8] or of the presence of RGS proteins on desensitization kinetics[29]. In a recent report, high concentrations of fatty acids, such as oleic and arachidonic acids, were shown to inhibit K_{ACh} currents[30]. The dependence of this effect on agonist-induced signalling and its involvement in current desensitization remain to be explored. Yet our results in native atrial cells, showing that a block on PLC activity dramatically attenuates desensitization, suggest that G-protein-stimulated PIP$_2$ hydrolysis by PLC is a major way in which K^+ currents desensitize in these cells. The precise contribution of distinct regulatory components of PIP$_2$ levels in the physiology of different cell types will undoubtedly be a major task of future research. □

© 2000 Macmillan Magazines Ltd

Methods

DNA subcloning, cRNA injection and reagents.

All cDNA constructs were subcloned in the pGEM-HE vector to generate transcripts for expression in oocytes[31]. RNA was transcribed *in vitro* using T7 polymerase (In Vitro mMessage mMachine kit, Ambion). The size and integrity of the cRNA was confirmed on formaldehyde agarose gels. Oocytes were injected with 1–3 ng of the channel subunits, hM_2, M_1 and 8 ng of EGFR cRNAs. The GFP-tagged PH domain of PLC-δ1 (PH–GFP) cDNA was kindly provided by Tobias Meyer (Duke University) and was subcloned in pcDNA3 for transfection in COS-1 cells and in pGEM-HE for expression in oocytes. U73122 was purchased from Calbiochem; it was dissolved in chloroform and aliquoted. The chloroform was evaporated under nitrogen. U73122 was stored at –20 °C and reconstituted in DMSO before use. ACh was purchased from Sigma, as were most of the common chemicals. EGF was purchased from Boehringer Mannheim.

Cell culture and transfection

Atrial cells were isolated from 3–5-day-old newborn rats as previously described[32]. The atrial cells were cultured in medium 199 supplemented with penicillin, streptomycin and 10% newborn calf serum. COS-1 cells were cultured in DMEM supplemented with penicillin, streptomycin and 10% fetal calf serum. For electrophysiological experiments COS-1 cells were transfected with the GIRK 1 and GIRK 4 cDNAs that were subcloned in the pcDNA 3 vector. These cells were also co-transfected with pEGFP (Clontech) for positive identification of transfected cells by fluorescence. For transfections we used the Effectene kit (Qiagen).

Electrophysiological measurements

Recordings in *Xenopus laevis* oocytes were made 2–5 days after cRNA injection. Currents were recorded using two-electrode voltage clamp (Dagan CA-1 amplifier). Electrodes were filled with 3 M KCl dissolved in 1% agarose. GIRK 1/GIRK4 or GIRK4(S143T)[33] (designated G4*) currents were recorded in ND96K solution (91 mM KCl, 1 mM NaCl, 1 mM $MgCl_2$ and 5 mM HEPES/KOH pH 7.4). In certain experiments (when indicated) oocytes were incubated for 3 h before recording GIRK channel activity with 1 μM thapsigargin and 1 mM EGTA to deplete endogenous calcium pools[34] and to eliminate the Ca^{2+}-activated Cl^- current during K^+ current recording. A voltage ramp protocol from –100 mV to 80 mV was applied at 1-s intervals and the currents corresponding to –80 mV were plotted as a function of time. At the end of the experiment, K^+ currents were blocked by 3 mM $BaCl_2$ or 10 mM CsCl in ND96K solution. GIRK currents in thapsigargin-treated oocytes were recorded in ND96K solution also containing 1 mM EGTA. Ca^{2+}-activated Cl^- currents were recorded in ND96 solution (96 NaCl, 2 mM KCl, 2 mM $MgCl_2$, 5 mM HEPES pH 7.4). In the experiments involving thapsigargin treatment, Ca^{2+}-activated Cl^- currents were recorded in ND96 solution containing 2 mM $BaCl_2$.

Whole-cell recordings in atrial and COS-1 cells were obtained with an Axopatch 200A amplifier (Axon Instruments). Voltage protocols were generated and data were digitized, recorded and analysed using HEKA software (Heka Electronik). Cell capacitance was determined by the whole-cell capacitance compensation circuit of the amplifier. Electrode resistances were 4–6 MΩ. The whole-cell recordings from COS-1 cells were carried out 48–72 h after transfection with the cDNAs of interest. The pipette solution contained (in mM): 110 potassium aspartate, 20 KCl, 10 NaCl, 1.0 $MgCl_2$, 2.0 MgATP, 0.1 GTP, 5.0 EGTA, 10 HEPES/KOH pH 7.4. The external solution contained (in mM): 140 KCl, 2.0 $CaCl_2$, 1.0 $MgCl_2$, 10 HEPES/KOH pH 7.4.

The QLKK peptide (single-letter amino acid notation) was composed of the following amino acids: QLKKLKEICEKEKKELKKKMDKKRQEKITEAK, while the ADRK peptide contained the following amino acids: ADRKRVETALEACSL. Both these peptides were prepared and used as described by Wu *et al.*[9].

Single-channel recording was performed as previously described[21,24]. Single-channel currents were filtered at 1 kHz with a 6-pole low-pass Bessel filter, sampled at 5 kHz. Single-channel data were analysed with pCLAMP 8 software supplemented with some of our own routines. Baseline drifts were carefully adjusted with Clampfit 8 before idealization. Only those records containing a few or no double openings were used for open-time histogram fitting. To increase the likelihood of encountering a small number of channels in the cell-attached patches, much less GIRK1/GIRK4 channel (0.2 ng cRNAs per oocyte) and hM_2 receptor (0.2 ng per oocyte) than M_1 receptor (4 ng per oocyte) were injected. Recordings were made 2 days after injection.

Confocal microscopy of albino *Xenopus* oocytes

The GFP-tagged PH domain of PLC-δ (GFP–PH) and EGFR were expressed in albino oocytes by cRNA injection as described above. Two to three days after injection, the oocytes were imaged using an upright Leica TCS NT confocal microscope. The oocytes were placed in a small chamber on a glass coverslip and placed on the microscope stage. A 1-μm section of the oocyte was imaged using a 10 × objective. EGF (100 ng ml^{-1}) was applied to the oocytes without disrupting the oocyte position in the chamber. A second confocal image was obtained from the same cross section 1 min following EGF application.

Confocal microscopy of COS-1 cells

The cells were grown on 40-mm diameter coverslips and transfected with the appropriate receptor constructs as described above. The GFP–PH construct was subcloned into pcDNA3 (Invitrogen) and co-transfected. Two days after transfection, the coverslips were mounted in a chamber (Bioptechs Corp.) designed for an inverted Leica TCS NT confocal Microscope. The cells were imaged using either a ×40 or ×100 oil objective. The cells were constantly perfused with normal extracellular solution except during image acquisition. Stopping the flow during image capture reduced movement of the cell in the *Z*-direction, enabling us to accurately capture the same cross-section of each cell repeatedly. Laser intensity and pinhole settings were kept constant between experiments. The perfusion was carried out by a peristaltic pump; the dead volume between the solution reservoirs and the chamber delayed drug application by 30 s and was taken into account for the kinetic analysis. Placing small air bubbles between different solutions in the tube prevented mixing of solutions in the perfusion tubing. Control images were obtained for 3 min before drug application. U73122 was applied for 3 min preceding the first ACh application. In the images shown, GFP–PH fluorescence is excluded by the nucleus of the COS-1 cells. We took multiple line scans, always excluding the nucleus. Regardless of the line scan, the measurements were always similar, which gave us confidence to show a single representative scan as well as summary data from three to six cells for each condition.

Fluorescent signal analysis

Images acquired using the confocal microscope were saved as TIFF files. The files were directly opened by Scion image processing software. A specific cross-section at a constant position with a constant width and length was chosen for each cell that was analysed. The fluorescence intensity profile was plotted for each cross-section. The intensity values were saved and transferred to Microsoft Excel for further analysis. Constant regions within the profile of each cell were designated as membrane, with areas in between as cytoplasm. The ratio of average fluorescence intensity of membrane to cytoplasm was calculated. The value for the last control measurement for each cell was designated as 100% and other time points were expressed as percent control.

RECEIVED 20 MARCH 2000; REVISED 25 APRIL 2000; ACCEPTED 18 MAY 2000; PUBLISHED 17 JULY 2000.

1. Kubo, Y., Reuveny, E., Slesinger, P. A., Jan, Y. N. & Jan, L. Y. Primary structure and functional expression of a rat G-protein-coupled muscarinic potassium channel. *Nature* **364,** 802–806 (1993).
2. Dascal, N., Schreibmayer, W., Lim, N. F., Wang, W., Chavkin, C., DiMagno, L., Labarca, C., Kieffer, B. L., Caveriaux-Ruff, C., Trollinger, D., Lester, H. A. & Davidson, N. Atrial G protein-activated K^+ channel: Expression cloning and molecular properties. *Proc. Natl Acad. Sci. USA* **90,** 10235–10239 (1993).
3. Krapivinsky, G., Gordon, E. A., Wickman, K., Velimirovic, B., Krapivinsky, L. & Clapham, D. E. The G-protein-gated atrial K^+ channel I_{KACh} is a heteromultimer of two inwardly rectifying K^+-channel proteins. *Nature* **374,** 135–141 (1995).
4. Caulfield, M. P. & Birdsall, N. J. M. Classification of muscarinic acetylcholine receptors. International Union of Pharmacology. XVII. *Pharmacol. Rev.* **50,** 279–290 (1998).
5. Logothetis, D. E., Kurachi, Y., Galper, J., Neer, E. J. & Clapham, D. E. The βγ subunits of GTP-binding proteins activate the muscarinic K channel in heart. *Nature* **325,** 321–326 (1987).
6. Krapivinsky, G., Krapivinsky, L., Wickman, K. & Clapham, D. E. Gβγ binds directly to the G protein-gated K^+ channel, I_{KACh}. *J. Biol. Chem.* **270,** 29059–29062 (1995).
7. Yamada, M., Inanobe, A. & Kurachi, Y. G protein regulation of potassium ion channels. *Pharmacol. Rev.* **50,** 723–757 (1998).
8. Kurachi, Y., Nakajima, T. & Sugimoto, T. Short-term desensitization of muscarinic K^+ channel current in isolated atrial myocytes and possible role of GTP-binding proteins. *Pflügers Arch.* **410,** 227–233 (1987).
9. Wu, D., Jiang, H., Katz, A. & Simon, M. I. Identification of critical regions on phospholipase C-beta 1 required for activation by G-proteins. *J. Biol. Chem.* **268,** 3704–3709 (1993).
10. Stauffer, T. P., Ahn, S. & Meyer, T. Receptor-induced transient reduction in plasma membrane PtdIns(4,5)P_2 concentration monitored in living cells. *Curr. Biol.* **8,** 343–346 (1998).
11. Varnai, P. & Balla, T. Visualization of phosphoinositides that bind pleckstrin homology domains: Calcium- and agonist-induced dynamic changes and relationship to myo-[^{3}H]inositol-labeled phosphoinositide pools. *J. Cell Biol.* **143,** 501–510 (1998).
12. Hirose, K., Kadowaki, S., Tanabe, M., Takeshima, H. & Masamitsu I. Spatiotemporal dynamics of inositol 1,4,5-triphosphate that underlies complex Ca^{2+} mobilization patterns. *Science* **284,** 1527–1530 (1999).
13. Yim, D. L., Opresko, L. L., Wiley, H. S. & Nuccitelli, R. Highly polarized EGF receptor tyrosine kinase activity initiates egg activation in *Xenopus*. *Dev. Biol.* **162,** 41–55 (1994).
14. Hilgemann, D. W. Cytoplasmic ATP-dependent regulation of ion transporters and channels: mechanisms and messengers. *Annu. Rev. Physiol.* **59,** 193–220 (1997).
15. Sui, J. L., Petit-Jacques, J. & Logothetis, D. E. Effect of phosphatidylinositol phosphates on the gating of G-protein-activated K^+ channels. *Curr. Topics Membranes* **46,** 337–354 (1999).
16. Hilgemann, D. W. & Ball, R. Regulation of cardiac Na^+, Ca^{2+} exchange and K_{ATP} potassium channels by PIP_2. *Science* **273,** 956–959 (1996).
17. Fan, Z. & Makielski, J. C. Anionic phospholipids activate ATP-sensitive potassium channels. *J. Biol. Chem.* **272,** 5388–5395 (1997).
18. Baukrowitz, T., Schulte, U., Oliver, D., Herlitze, S., Krauter, T., Tucker, S. J., Ruppersberg, J. P. & Fakler, B. PIP_2 and PIP as determinants for ATP inhibition of K_{ATP} channels. *Science* **282,** 1141–1144 (1998).
19. Shyng, S.-L. & Nichols, C. G. Membrane phospholipid control of nucleotide sensitivity of K_{ATP} channels. *Science* **282,** 1138–1141 (1998).
20. Huang, C.-L., Feng, S. & Hilgemann, D. W. Direct activation of inward rectifier potassium channels by PIP_2 and its stabilization by Gβγ. *Nature* **391,** 803–806 (1998).
21. Sui, J.-L., Petit-Jacques & Logothetis, D. E. Activation of the atrial K_{ACh} channel by the βγ subunits of G proteins or intracellular Na^+ ions depends on the presence of phosphatidylinositol phosphates. *Proc. Natl Acad. Sci. USA* **95,** 1307–1312 (1998).
22. Zhang, H., He, C., Yan, X., Mirshahi, T. & Logothetis, D. E. Specific PIP_2 interactions with inwardly rectifying K^+ channels determine distinct activation mechanisms. *Nature Cell Biology* **1,** 183–188 (1999).
23. Liou, H. H., Zhou, S. S. & Huang, C. L. Regulation of ROMK 1 channel by protein kinase A via a phosphatidylinositol 4,5-bisphosphate-dependent mechanism. *Proc. Natl Acad. Sci. USA* **96,** 5820–5825 (1999).
24. Sui, J. L., Chan, K. W. & Logothetis, D. E. Na^+ activation of the muscarinic K^+ channel by a G-protein-independent mechanism. *J. Gen. Physiol.* **108,** 381–391 (1996).
25. Petit-Jacques, J., Sui, J.-L. & Logothetis, D. E. Synergistic activation of GIRK channels by Na^+, Mg^{2+} and Gβγ subunits. *J. Gen. Physiol.* **114,** 673–684 (1999).
26. Ho, I. H. M. & Murrell-Lagnado, R. D. Molecular mechanism for sodium dependent activation of G protein-gated K^+ channels. *J. Physiol.* **520,** 645–651 (1999).
27. Logothetis, D. E. & Zhang, H. Gating of G protein-sensitive inwardly rectifying K^+ channels through phosphatidylinositol 4,5-bisphosphate. *J. Physiol.* **520,** 630 (1999).
28. Xie L.-H., Horie, M. & Takano M. Phospholipase C-linked receptors regulate the ATP-sensitive potassium channel by means of phosphatidylinositol 4,5-bisphosphate metabolism. *Proc. Natl Acad. Sci. USA* **96,** 15292–15297 (1999).
29. Chuang, H.-H., Yu, M., Jan, Y. N. & Jan, L. Y. Evidence that the nucleotide exchange and hydrolysis cycle of G proteins causes acute desensitization of G-protein gated inward rectifier K^+ channels. *Proc. Natl Acad. Sci. USA* **95,** 11727–11732 (1998).
30. Kim, D. & Pleumsamran, A. Cytoplasmic unsaturated free fatty acids inhibit ATP-dependent gating

 © 2000 Macmillan Magazines Ltd

of the G protein-gated K^+ channel. *J. Gen. Physiol.* **115,** 287–304 (2000).
31. Liman, E. R., Tytgat, J. & Hess, P. Subunit stoichiometry of a mammalian K^+ channel determined by construction of multimeric cDNAs. *Neuron* **9,** 861–871 (1992).
32. Muir, T. M., Hair, J., Inglis, G. C., Dow, J. W., Lindop, G. B. M. & Leckie, B. J. Dexamethasone-induced differentiation of atrial myocytes in culture. *Am. J. Physiol.* **263,** H 722–H 729 (1992).
33. Vivaudou, M., Chan, K. W., Sui, J. L. Jan L.Y., Reuveny, E. & Logothetis, D. E. Probing the G-protein regulation of GIRK 1 and GIRK 4, the two subunits of the K_{ACh} channel, using functional homomeric mutants. *J. Biol. Chem.* **272,** 31553–31560 (1997).
34. Petersen, C. C. & Berridge, M. J. The regulation of capacitative calcium entry by calcium and protein kinase C in *Xenopus* oocytes. *J. Biol. Chem.* **269,** 32246–32253 (1994).

ACKNOWLEDGEMENTS
We are grateful to X. Yan for preparation of oocytes, S. Henderson for help with the confocal experiments, and I. Wolf for peptide synthesis. We thank H. S. Wiley (University of Utah), X-Y. Huang (Cornell University Medical College) and T. Meyer (Duke University) for their kind gifts of EGF receptor, M_1 receptor and GFP–PH cDNAs, respectively. We also thank R. Anderson, D. Clapham, M. Greenberg, R. Iyengar, R. Margolskee, S. Sealfon, M. Ming Zhou and members of the Logothetis lab for critical comments on the manuscript. This work was supported by grants to D.E.L. from the NIH (HL54185 and HL59949). T.M. was supported by NIH Training Grant DK 07757 and a Charles H. Revson fellowship.
Correspondence and requests for materials should be addressed to D.E.L.

© 2000 Macmillan Magazines Ltd